

A 3-D Heat Transfer Model for MR Signal Dependence on Flying Height and Its Application

Li Chen and David B. Bogy

Computer Mechanics Laboratory, University of California, Berkeley, CA 94720

Shuyu Zhang

Iomega Corporation, CA 95035

ABSTRACT

A 3-D heat transfer model for the slider body is developed to study the MR read back signal dependence on slider flying height as well as its response after thermal disturbances. The bias current in the MR sensor raises the temperature in the MR element to a value much higher than the ambient temperature. The air bearing acts as a coolant that transfers heat from the slider to the disk, but this cooling effect decreases with the increase of the flying height, so the temperature distribution in the slider will be affected by the flying height. With a typical current value of around 10 mA in the MR sensor, our simulation predicts a steady state MR temperature that is about 40 °C hotter than ambient. Using the model, we find that the temperature distribution inside the MR element depends significantly on the slider-disk spacing at the gap, while it shows a weak dependence on the slider's pitch and roll. Two classes of thermal interference events are simulated; first is the "baseline wander" caused by increased cooling when the sensor passes over an asperity near contact, and the other is the "thermal asperity" resulting from frictional heating by asperity-sensor contacts.

Keywords: MR element, air bearing, thermal interference, thermal asperity

1. Introduction

Since MR sensors are exposed at the air bearing surface, and the MR read back signal depends significantly on MR temperature, thermal interference (TI) events occasionally occur. These TI events can cause perturbations that last long enough to overdrive and saturate the recording channel, resulting in error bursts. There have been several studies of the heat transfer mechanism related to MR read back signal disturbances in hard disk drives.

Zhang and Bogoy (1997) studied the heat transfer between the slider and air bearing, and they derived the expression for heat flux between them using simplified momentum and energy equations in the air bearing. Later Zhang and Bogoy (1998) developed a 2-D heat conduction model for the slider body, assuming that the MR sensor together with its shields provide the heat source with uniform heat generation Q_0 . They assumed that the MR head was embedded in a large thin plate as shown in Fig. 1(a), and the heat Q_0 was transferred in the slider plate and to the air bearing.

Since the thickness of the MR sensor is about $3\mu\text{m}$ while the thickness of the pico slider is about 0.4 mm, and the construction of the MR sensor together with its shields is also quite complex (as shown in Fig.2), a 3-D model is necessary to accurately calculate the temperature in the MR sensor. In this report, we develop a 3-D heat transfer model in the slider. The diagram is shown in Fig. 1(b). The side view and the top view of the MR element are shown in Figs. 2 (a) and (b). The heat source in the slider is the heat caused

by the bias current inside the MR sensor. The size of the MR sensor is 10 μm x 50 nm x 4 μm . Heat will be transferred to the shields and then to other parts of the slider and the air bearing. With this model we obtain steady state MR temperatures versus bias current and flying height. We also simulate two classes of TI events; the “baseline wander” caused by increased cooling when the sensor passes over an asperity near contact, and the “thermal asperity” resulting from frictional heating by asperity-sensor contacts.

2. 3-D Heat Transfer Model in the Slider

(1) Governing equation

The governing equation for the 3-D unsteady heat conduction problem in the slider is written as follows:

$$\rho c \frac{\partial T}{\partial \tau} = \frac{\partial}{\partial x} \left(k \frac{\partial T}{\partial x} \right) + \frac{\partial}{\partial y} \left(k \frac{\partial T}{\partial y} \right) + \frac{\partial}{\partial z} \left(k \frac{\partial T}{\partial z} \right) + S, \quad (1)$$

where ρ , c and k are, respectively, density, specific heat and thermal conductivity of the slider, T is the temperature difference between the slider plate and the ambient, τ is the time, and x , y and z are coordinates in the slider. Since the slider is composed of different materials the physical properties are not uniform. The source term S (unit: W/m^3) can be expressed as:

$$S = \begin{cases} Q_0 \left(= \frac{I_s^2 R_s}{V_s} \right), & (x, y, z) \in \Gamma_s \\ 0, & \text{otherwise} \end{cases} \quad (2)$$

where, I_s , R_s , V_s and Γ_s are, respectively, bias current, electrical resistance, volume and the domain of the MR sensor.

(2) Boundary conditions

The air flows over the disk due to its rotation. Due to centrifugal force, the air flow will have a radial component and then an axial component to fill in. The boundary layer thickness of the air flow is (White, 1991):

$$\delta = 5 \sqrt{\frac{\nu}{\omega}}, \quad (3)$$

where ν and ω are the kinetic viscosity of the air and the disk rotation speed respectively. The kinetic viscosity of air is $15.89 \times 10^{-6} \text{ m}^2/\text{s}$, and when the disk rotation is 5400 rpm, ω is about 550 rad/s. So δ is about 0.8 mm. Since the thickness of slider is about 0.4 mm, the slider is immersed in the boundary layer. We can use boundary layer theory (Kays, and Crawford, 1993) to determine the heat convection coefficient of the heat transfer between the surrounding air and the slider. In the boundary layer, the Nusselt number can be determined from the Reynolds number Re and the Prandtl number Pr :

$$N_u = \frac{h_{con} L}{k} \sim \sqrt{Re \cdot Pr}, \quad (4)$$

where h_{con} , L and k are the heat convection coefficient, the characteristic length of the disk and the heat conduction coefficient, respectively. At a radius of 40 mm with the disk rotation of 5400rpm the velocity is about 20m/s, so $Re = \frac{uL}{\nu} \sim 10^5$. Under ambient temperature and pressure, the Prandtl number of air is 0.7, and the heat conduction coefficient k of air is $26.3 \times 10^{-3} \text{ w/m}\cdot\text{K}$. Then from equation (4) we conclude that h_{con} is on the order of $100 \text{ w/m}^2\cdot\text{k}$.

The heat resistance of the air flow per unit area is: $\frac{1}{h_{con}} \sim 10^{-2} (k/w)$

The heat resistance of the slider per unit area is: $\frac{L_{sli}}{k} \sim 10^{-5} (k/w)$

The heat resistance of the suspension per unit area is: $\frac{L_{sus}}{k} \sim 10^{-7} (k/w)$

Thus the heat resistance of air flow is more than 1000 times greater than that of the slider and the suspension, so we can regard the boundary at the top and side surfaces of the slider as adiabatic.

At the air bearing-slider interface heat will be transferred from the slider to the disk through the air bearing cooling effect. This is a micro-structure quasi-steady heat transfer problem. Zhang and Bogoy (1998a) obtained the heat flux between the slider and the slider-disk interface, which is expressed as follows:

$$q = -k_a \frac{T}{h + 2b\lambda_a} + \frac{h^3}{24\mu_a} \left[\left(\frac{\partial p}{\partial \xi} \right)^2 + \left(\frac{\partial p}{\partial \eta} \right)^2 \right] + \frac{\mu_a U^2 h}{2(h + 2a\lambda_a)^2} - \frac{Uh^3}{6(h + 2b\lambda_a)(h + 2a\lambda_a)} \frac{\partial p}{\partial \xi}, \quad (5)$$

where, ξ and η are coordinates in the air bearing, k_a , μ_a and λ_a are, respectively, the thermal conductivity, viscosity and mean-free-path of the air, T is the temperature difference between the slider bottom surface and the disk surface (we assume the disk surface has the same temperature as the ambient), U is the local velocity of the disk, h is the air bearing spacing, $a=(2-\sigma_M)/\sigma_M$ and $b=2(2-\sigma_T)\gamma_a/\sigma_T(\gamma+1)Pr_a$, where σ_M is the momentum accommodation coefficient and σ_T is the thermal accommodation coefficient,

γ_a is the ratio of specific heats at constant pressure and constant volume, and Pr_a is the Prandtl number of the air.

We can write equation (5) in a simpler form as: $q=AT+B$, where A is the coefficient of the 1st term and B is the rest of the terms on RHS.

3. Integration of the Conduction Equation

We use Patankar's (1980) control volume method to integrate the heat conduction equation (1). A 2-D control volume is depicted in Fig. 3, where the shaded area is the control volume, and Δx and Δy are the lengths of its two edges. The capital letters E, S, W, N and P represent the grid nodes and small letters e, s, w and n represent the related control volume surfaces. The 3-D control volume is quite similar to that in 2-D, but it has two more related control surfaces perpendicular to the z direction, denoted as u and l , which mean upper and lower.

Now integrating equation (1) over the control volume and time, we get:

$$\begin{aligned} \int_{\tau}^{\tau+\Delta\tau} \int_l^u \int_s^n \int_w^e \rho c \frac{\partial T}{\partial \tau} dx dy dz d\tau &= \int_{\tau}^{\tau+\Delta\tau} \int_l^u \int_s^n \int_w^e \frac{\partial}{\partial x} \left(k \frac{\partial T}{\partial x} \right) dx dy dz d\tau + \\ &\int_{\tau}^{\tau+\Delta\tau} \int_l^u \int_s^n \int_w^e \frac{\partial}{\partial y} \left(k \frac{\partial T}{\partial y} \right) dx dy dz d\tau + \\ &\int_{\tau}^{\tau+\Delta\tau} \int_l^u \int_s^n \int_w^e \frac{\partial}{\partial z} \left(k \frac{\partial T}{\partial z} \right) dx dy dz d\tau + \int_{\tau}^{\tau+\Delta\tau} \int_l^u \int_s^n \int_w^e S dx dy dz d\tau \end{aligned} \quad (6)$$

Expanding (6) and re-arranging it yields:

$$a_p T_p = a_E T_E + a_W T_W + a_N T_N + a_S T_S + a_U T_U + a_L T_L + a_{P0} T_{P0} + b. \quad (7)$$

Equation (7) is in an implicit form and T_{P0} represents the temperature values at the last time step iteration. The related coefficients for the inner control volumes are:

$$a_p = a_E + a_W + a_S + a_N + a_U + a_L + a_{p0} \quad (8-a)$$

$$a_E = k_e \frac{\Delta y \Delta z}{(\delta x)_e} \quad (8-b)$$

$$a_W = k_w \frac{\Delta y \Delta z}{(\delta x)_w} \quad (8-c)$$

$$a_N = k_n \frac{\Delta x \Delta z}{(\delta y)_n} \quad (8-d)$$

$$a_S = k_s \frac{\Delta x \Delta z}{(\delta y)_s} \quad (8-e)$$

$$a_U = k_u \frac{\Delta x \Delta y}{(\delta z)_u} \quad (8-f)$$

$$a_L = k_l \frac{\Delta x \Delta y}{(\delta z)_l} \quad (8-g)$$

$$a_{p0} = \frac{\rho c_p \Delta x \Delta y \Delta z}{\Delta \tau} \quad (8-h)$$

$$b = S \Delta x \Delta y \Delta z \quad (8-i)$$

and k_e , k_w , k_n , k_s , k_u and k_l are, respectively, the thermal conductivity at each edge of the control volume.

For the boundary control volumes at the air bearing interface, the coefficients are:

$$a_p = a_E + a_W + a_S + a_N + a_U + a_L + a_{p0} - A \Delta x \Delta y \quad (9-a)$$

$$a_E = k_e \frac{\Delta y \Delta z}{2(\delta x)_e} \quad (9-b)$$

$$a_W = k_w \frac{\Delta y \Delta z}{2(\delta x)_w} \quad (9-c)$$

$$a_N = k_n \frac{\Delta x \Delta z}{2(\delta y)_n} \quad (9-d)$$

$$a_s = k_s \frac{\Delta x \Delta z}{2(\delta y)_s} \quad (9-e)$$

$$a_U = k_u \frac{\Delta x \Delta y}{(\delta z)_u} \quad (9-f)$$

$$a_L = 0 \quad (9-g)$$

$$a_{p0} = \frac{\rho c_p \Delta x \Delta y \Delta z}{2\Delta \tau} \quad (9-h)$$

$$b = \left(\frac{S}{2} + \frac{B}{\Delta z} \right) \Delta x \Delta y \Delta z \quad (9-i)$$

where A and B are terms in equation (5).

4. Numerical Approaches

In order to determine the heat flux q from the slider to the air bearing, we must first find the pressure distribution p in the air bearing as required by equation (5). For a steady flying state the pressure distribution can be obtained by solving the Reynolds equation (Lu, and Bogoy , 1997). For an unsteady flying state, such as a slider flying over an asperity, the pressure distribution is obtained by use of a dynamic slider air bearing analysis (Hu and Bogoy, 1997). Since the heat transfer in the interface is quasi-steady (Zhang and Bogoy, 1998), equation (5) can be used to calculate the heat flux at each transient flying state.

After the heat flux q is obtained the coefficients in equation (6) can be determined for each grid point, and the temperature distribution in the slider can be solved for at each time step. To solve the matrix from equation (7), we use the alternating direction line sweep method and tri-diagonal matrix algorithm.

After we determine the temperature variation we can calculate the MR signal change. There is a linear relationship between the MR temperature rise ΔT and the electrical resistance change ΔR (Tian, et al, 1997) : $\Delta T = \Delta R / (\alpha R_0)$, where R_0 and α are the initial resistance and the temperature coefficient of the MR sensor, respectively. The value of α is 0.00239K^{-1} , and the expression for the MR voltage is: $V = I(R_0 + \Delta R)$, where I is the bias current.

It's worth mentioning that we use very fine grids at the MR element due to its small size, with coarser grids farther from the MR element.

5. Simulation Results

We used a 50% (2 mm \times 1.6 mm) tri-pad slider in the following analysis. This slider has a taper angle and length of 0.01 *rad* and 0.2 *mm*, respectively, and a recess depth of 3 μm . It flies at the position of 23 mm from the center of the disk while the disk rotates at 5400 rpm. Its rail shape is shown in Fig. 4(a). The steady state flying characteristics are solved using the CML Air Bearing Design Code (Lu and Bogy , 1995) and are shown in Table 1.

Table 1. Flying characteristics of the tri-pad slider

Position r (mm)	Skew (degree)	Pitch (μ rad)	Roll (μ rad)	FH-CTE [‡] (nm)
23	8.0°	155.4	29.5	29.7

[‡]Flying height at the central trailing edge

Figure 4(b) shows the temperature distribution in the slider on one cross-section through the MR sensor when the slider is in a steady flying state. The bias current and

electric resistance in the MR sensor are 10 mA and 25 Ω respectively. The peak value in Fig. 4(b) corresponds to the MR temperature, about 42 °C above ambient.

5.1 MR Temperature Response for Different Flying Heights

When the slider's flying height is fixed at a different value, we can also use the air bearing code to obtain the pressure field in the air bearing, and then determine the MR temperature at that different flying height. Figure 5 is the plot of MR output signal versus flying height. It is shown that the MR voltage increases with flying height. This is because the cooling effect of the air bearing decreases with the increase of slider disk spacing. When the flying height increases from 40nm to 800nm, the MR voltage change is 3%. Our simulation results also show that the MR element temperature almost doesn't change with slider pitch or roll.

5.2 MR Temperature versus Bias Current

The MR temperature depends significantly on the bias current. Figure 6 shows the MR temperature above ambient versus bias current when the slider is in a steady flying state. We see that when the bias current increases from 8 mA to 20 mA, the calculated MR temperature increases from 30 °C to about 160 °C. Currently, the only experimental data available to us on the MR temperature dependence on bias current is a plot in the paper by Tian, et al, (1997), for which the ABS design was not available. According to our simulation results the MR temperature change with rail shape and flying height is very little compared to that with bias current, or MR size or electric resistance. Since the value of the MR size and electric resistance used in our calculation is on the same order of MR elements manufactured today, it's reasonable that we make a comparison of our

simulation results of MR temperature versus bias current with the experimental results in Fig.6. While the comparison may not be accurate, it shows that our simulation results are on the same order and in the same trend as the experimental results. We'll make more accurate comparisons in our future work.

5.3 MR Temperature Response for the Slider Flying Over An Asperity without Contact (Baseline Wander)

When the slider passes over an asperity, the slider disk spacing fluctuates. This causes the heat flux in the air bearing to also fluctuate, and so the MR signal will fluctuate. In order to show the relationship between the MR signal and the spacing during such a process we plot the MR temperature and the air bearing spacing at the MR sensor in the same figure (Fig. 7). In our calculation, the size of the asperity is 40 nm high, 80 μm long and 200 μm wide.

It is clearly shown that the MR temperature fluctuates following the same trend as the air bearing spacing. In the spacing history, the valley with minimum spacing of about 5 nm corresponds to the spacing when the slider just passes over the asperity. At this moment, the slider is near contact with the disk, and much more heat is transferred from the MR sensor to the disk, so there is a simultaneous drop in the MR temperature. The value of this temperature decrease is 0.04 $^{\circ}\text{C}$ and it is estimated to cause the MR read back signal to change by about 2%.

5.4 MR Temperature Response for a Slider Coming into Contact with an Asperity (Thermal Asperity)

The contact process is very complex and there are many models for calculating contact force. Here we simplify the case by assuming that the contact force is uniform and the

normal stress equals the yield strength. So the heat per unit area caused by friction is: $q=fvp$, where f is the friction coefficient, v is the velocity, and p is mean normal stress. We assume the heat caused by friction will diffuse into the slider and the asperity, respectively, according to the ratio of their heat conduction coefficients. The simulation results of the MR signal response of this process are shown in Fig. 8.

It is shown that before the asperity comes into contact with the MR element, the friction heat has little effect on the MR temperature. But when the asperity comes into contact with the MR element, there is a sharp rise of MR temperature, causing a related rise in voltage. Our simulated results of this peak temperature rise is about 5 °C, giving a voltage rise of 1.6 volts which is on the same order as measured results (Stupp, et al, 1998). The rise time is on the order of 0.1 μ s. After the asperity leaves the MR element, the MR temperature decays slowly in an exponential manner. The trend and time scale of the simulation results are very consistent with measured laser experiments (Stupp, et al, 1998).

6. Conclusion

The MR read back signal, which is closely related to the MR temperature, depends on the flying height of the slider. It can also be affected by thermal interference including the fluctuation of the heat transfer in the air bearing and friction during slider disk contact. We developed an unsteady 3-D heat transfer model to study the signal dependence on flying height and its response to thermal disturbances.

The simulation results show that the MR temperature increases from 30 °C to 160 °C when the bias current increases from 8 mA to 20 mA, and the MR temperature increases

about 15 °C when the flying height increases from 30 nm to 1 μm. The MR temperature is insensitive to slider pitch and roll.

The simulation results of the “baseline wander” event show that the MR temperature response has a sharp decrease when the MR element just passes the asperity, and then damps to its steady state value. The sharp decrease of temperature happens simultaneously with that of the air bearing spacing. This is caused by the cooling effect of the air bearing. With the given MR current and resistance as well as the size of the asperity, the maximum MR temperature variation is about 0.04 °C, which is estimated to cause the MR read back signal to change by about 2%.

The simulation results of the TA trend show that when the MR element comes into contact with an asperity, the MR temperature increase sharply on a time scale of 0.1μs, and then decreases exponentially. The peak temperature rise is several degrees. Since the simulation of the TA event was quite simplified in this report, a better contact model as well as a better heat transfer model at the contact interface needs to be used to obtain more reliable results.

Since the length of the MR element is on the order of a micrometer, and the width of MR sensor is less than 100 nm, a micro-scale heat transfer treatment which applies quantum theories may be required for a complete understanding.

References

Hu, Y., and Bogy, D. B., 1997, “Dynamic Stability and Spacing Modulation of Sub-25 nm Fly Height Sliders”, *ASME Journal of Tribology*, Vol.119, pp646-652.

Jander, A., Indeck, R. S., Brug, J. A., and Nickel, J. H., 1996, "A Model for Predicting Heating of Megnetoresistive Heads", *IEEE Transactions on Magnetics*, Vol.32, N.5, p3392-3394.

Kays, W. M., and Crawford, M. E., 1993, *Convective Heat and Mass Transfer*, McGraw-Hill, New York.

Lu, S., and Bogy, D. B., 1995, "CML Air Bearing Design Program User's Manual", *CML report*, No. 95-003, UC Berkeley.

Lu, S., 1997, *Numerical Simulation of Slider Air Bearing*, Doctoral Dissertation, Department of Mechanical Engineering, University of California, Berkeley.

White, F. M., 1991, *Viscous Fluid Flow*, McGraw-Hill, New York

Patankar, S. V., 1980, *Numerical Heat Transfer and Fluid Flow*, McGraw-Hill, New York.

Tian, H., Cheung, C-Y., and Wang, P-K., 1997, "Non-Contact Induced Thermal Disturbance of MR Head Signals", *IEEE Transactions on Magnetics*, Vol.33, No.5, pp3130-3132.

Zhang, S., Bogy, D. B., 1997, "A Heat Transfer Model for Thermal Fluctuation in a Thin Air Bearing", *International Journal of Heat and Mass Transfer*, Vol.42, pp1791-1800.

Zhang, S., and Bogy, D. B., 1998, "Variation of the Heat Flux between a Slider and the Air Bearing when the Slider Flies over an Asperity", presented in the *INTERMAG98*, and to appear in *IEEE Transactions on Magnetics*.

Zhang, S., and Bogy, D. B., 1998, "Temperature Response of A MR Head When it Flies Over An Asperity", *CML report*, No. 98-001, UC Berkeley.

Stupp, S., McEwen, P., and Boldwinson, M., June 1998, "Thermal Asperity Model Shows Growing Threat", *Data Storage*, pp31-32.

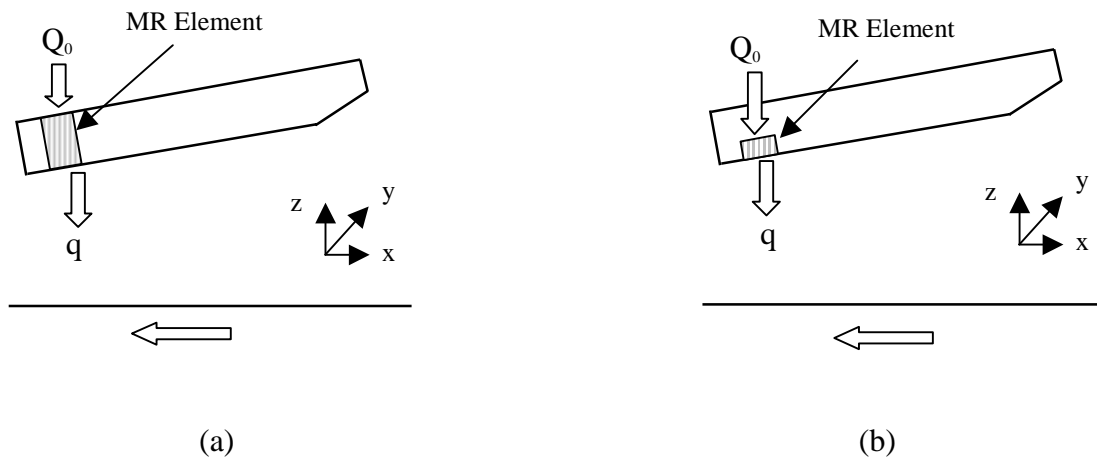


Fig. 1 Diagrams for the 2-D (a) and 3-D (b) heat transfer model

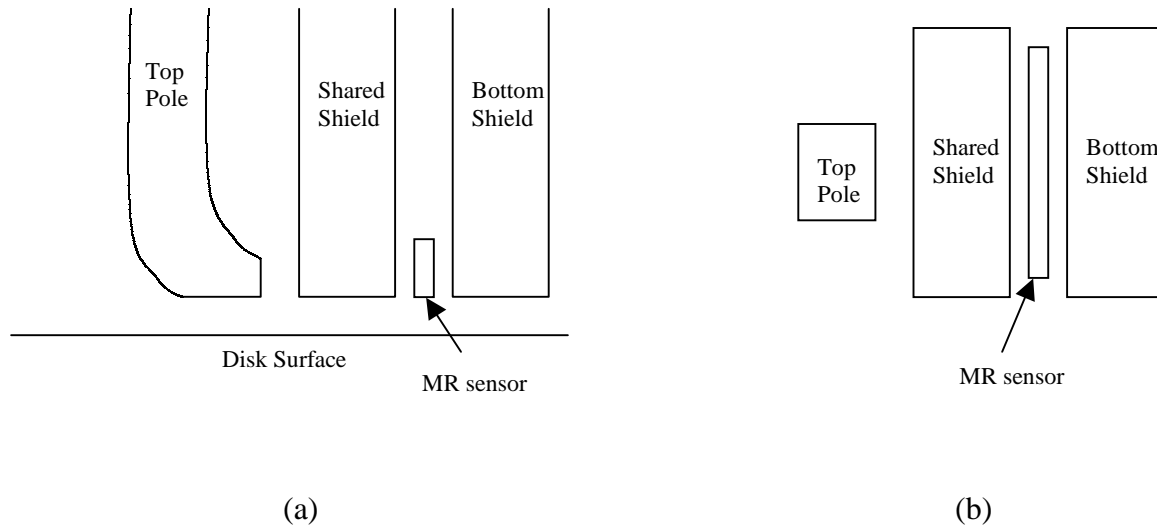


Fig.2 Side view (a) and top view (b) of MR element

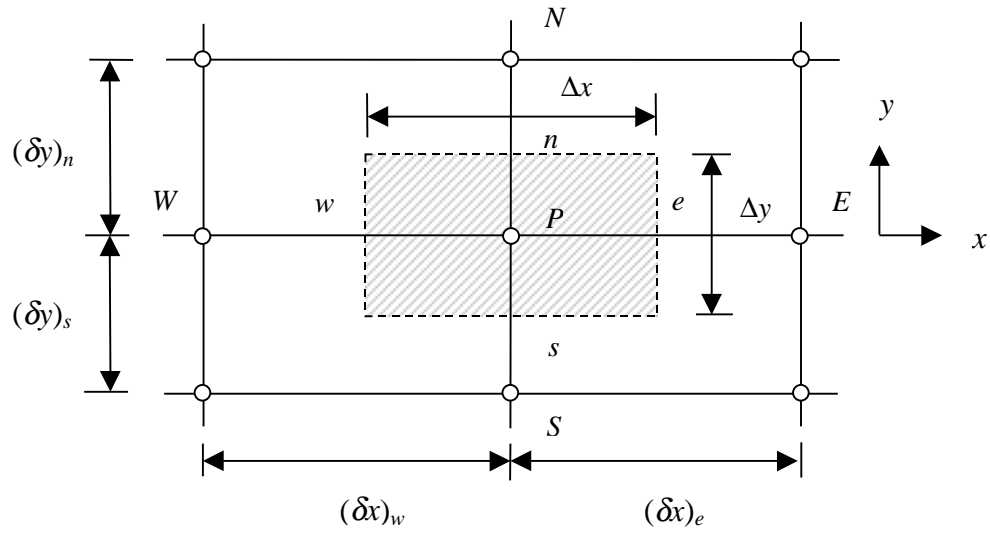


Fig. 3 Diagram of the 2-D control volume

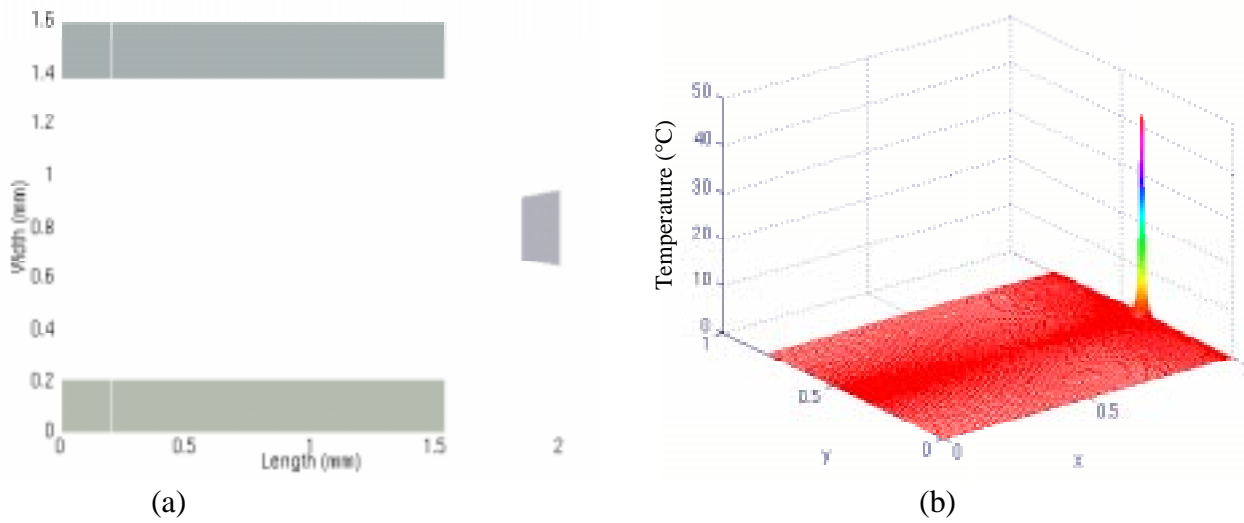


Fig. 4 Rail shape (a) and temperature profile (b) of the slider studied

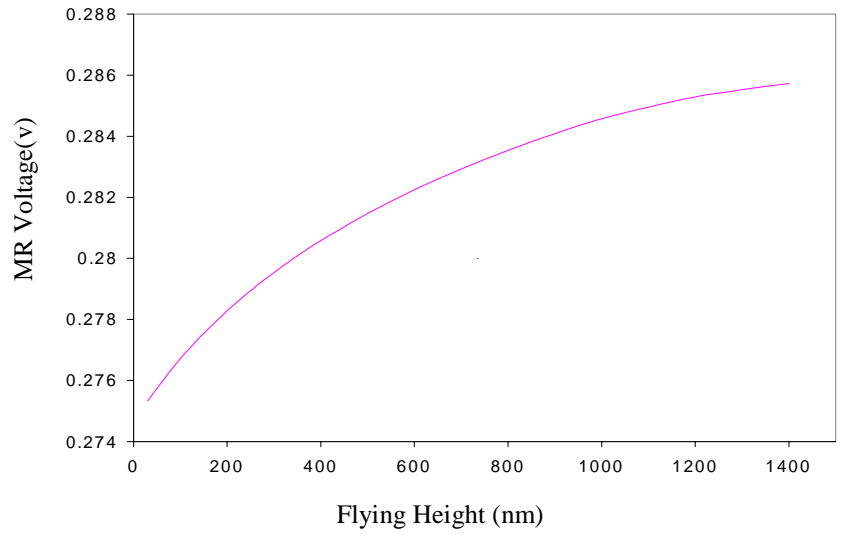


Fig. 5 MR signal versus flying height

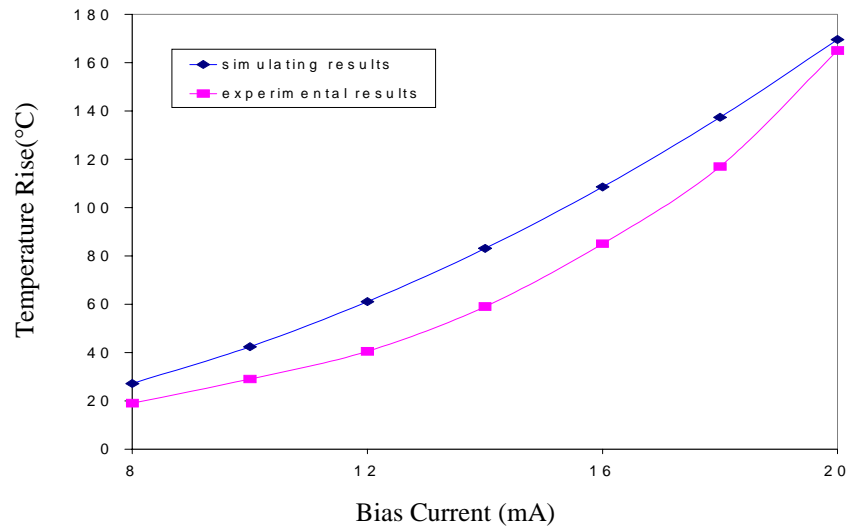


Fig. 6 MR temperature dependence on bias current.

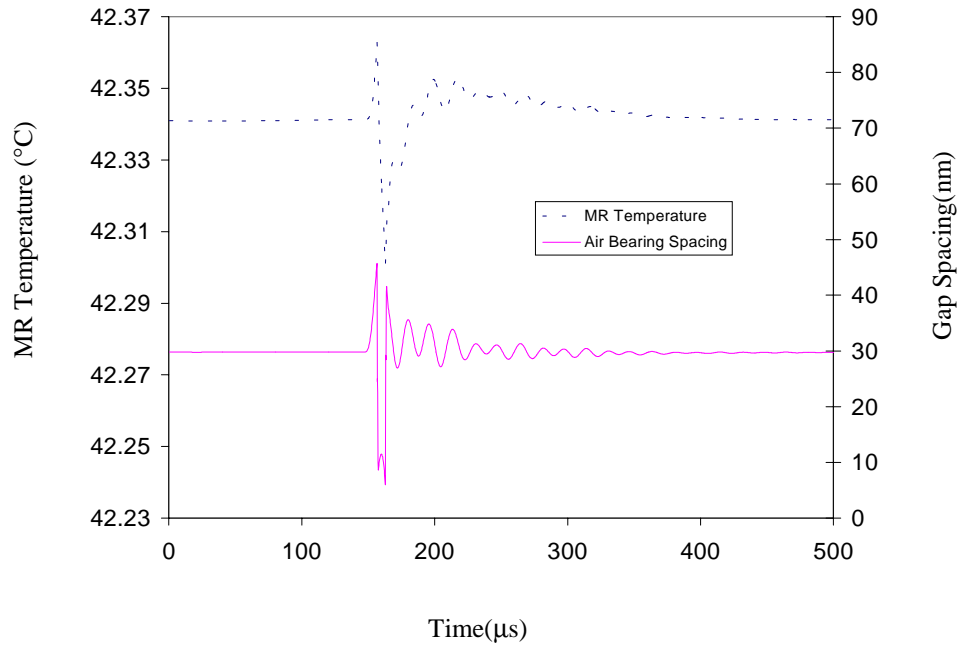


Fig. 7 MR temperature response when slider flies over an asperity without contact

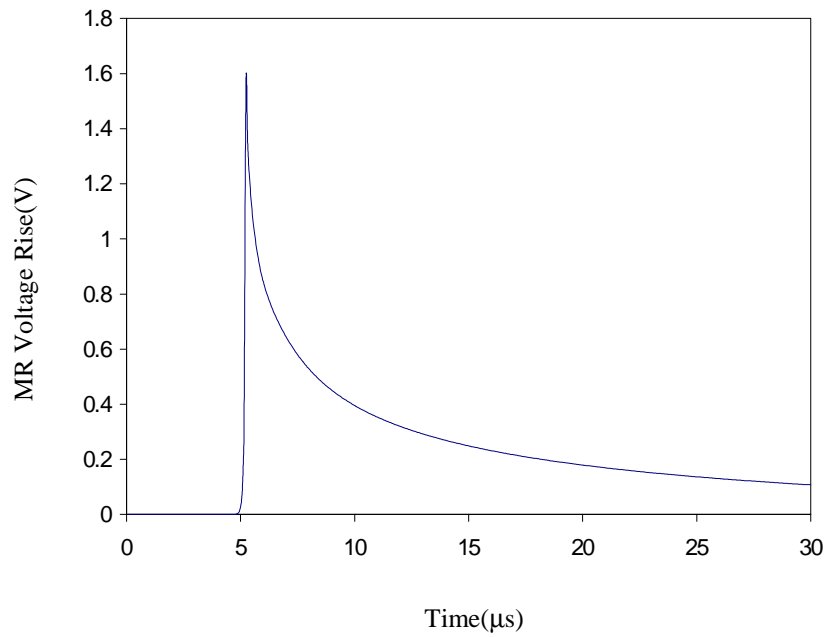


Fig. 8 MR response during TA event